Liquid Crystals
Publication details, including instructions for authors and subscription information:
http://www.informaworld.com/smpp/title~content=t713926090

Short chain copper(II) *n*-alkanoate liquid crystals

J. A. R. Cheda Corresponding author[a]; M. V. García[a]; M. I. Redondo[a]; S. Gargani[b]; P. Ferloni[b]
[a] Departamento de Química Física, Facultad de Ciencias Químicas, Universidad Complutense, 28040 Madrid, Spain [b] Dipartimento di Chimica Fisica and CSTE-CNR, Università di Pavia, 27100 Pavia, Italy

To cite this Article Cheda Corresponding author, J. A. R. , García, M. V. , Redondo, M. I. , Gargani, S. and Ferloni, P.(2004) 'Short chain copper(II) *n*-alkanoate liquid crystals', Liquid Crystals, 31: 1, 1 — 14
To link to this Article: DOI: 10.1080/02678290310001628500
URL: http://dx.doi.org/10.1080/02678290310001628500

Liquid Crystals, Vol. 31, No. 1, January 2004, 1–14

Taylor & Francis
Taylor & Francis Group

Short chain copper(II) *n*-alkanoate liquid crystals

J. A. R. CHEDA*, M. V. GARCÍA, M. I. REDONDO
Departamento de Química Física, Facultad de Ciencias Químicas, Universidad Complutense, 28040 Madrid, Spain

S. GARGANI and P. FERLONI
Dipartimento di Chimica Fisica and CSTE-CNR, Università di Pavia, Viale Taramelli 16, 27100 Pavia, Italy

(*Received 23 April 2003; in final form 21 July 2003; accepted 16 August 2003*)

Four short chain members of the copper(II) *n*-alkanoate series Cu(C*n*)$_2$, from propanoate to hexanoate, have been synthesized, purified and characterized by means of optical microscopy, thermogravimetric analysis (TGA), differential scanning calorimetry (DSC), FTIR and Raman spectroscopy. The TGA study shows that decomposition starts on heating above 420–470 K (depending on the sample) in a nitrogen atmosphere. In addition, thermal decomposition was investigated by DSC using special high pressure pans and endo- and exothermic processes were found which have not been reported previously. All but one of the compounds melt to a liquid crystal phase, which decomposes before the clearing point. The exception is the propanoate homologue, which decomposes directly from the solid state. Despite this problem of sample decomposition, the identification by optical microscopy of the tetragonal (butanoate) and hexagonal (pentanoate and hexanoate) discotic columnar phases was, for first time, possible by the addition of small amounts of the corresponding acid to the samples. These results are in agreement with the X-ray diffraction study performed using swelled mixtures of these salts with hydrocarbon solvents. Two solid–solid transitions, not previously reported in the literature, were found for the butanoate homologue at 395.9 and 422.9 K with $\Delta H = 8.27$ and $1.37\,\mathrm{kJ\,mol^{-1}}$, respectively. The solid and liquid crystalline phases were investigated using variable temperature FTIR spectroscopy.

1. Introduction

Several families of ionic organic materials, such as alkali and alkaline earth metal alkanoates with either linear or branched hydrocarbon chains, have been the focus of many recent studies, either for fundamental reasons or for a wide variety of scientific and industrial applications. Previous information on the chemical and physical properties of these materials has been collected in a number of reviews, among which the book edited by Franzosini and Sanesi [1] and the survey by Mirnaya *et al.* [2] are worthy of mention. This family of organic salts has been considered as a part of the most general family of metallomesogens, as it appears in the recent review by Donnio [3].

Within this framework, the di-copper(II) *n*-alkanoates Cu(C*n*)$_2$ (*n* = number of carbons in each carboxylate chain) represent a series of organic compounds that may be considered of great interest from various standpoints. The members with long chain anions find a variety of practical uses as components of dye mixtures, as stabilizers in polymeric materials, and in lubricants. The short chain homologues, among which the acetate is the best known, are employed, for example, as catalysts in organic reactions, and may be viewed as model molecules in the composition of green colour in ancient paintings. Moreover, copper complexes formed with carboxylate units are widely present in living systems, and attract much attention because of their biological and pharmaceutical activity [4].

Structural data have been obtained by means of X-ray diffraction (XRD) for the butanoate [5, 6], hexanoate [7] octanoate [8 *a*] and decanoate [8 *b*] homologues by various authors. All the data confirm the existence of a central core with pairs of copper ions bridged by four *n*-alkyl chains, two of which are in the all-*trans* conformation; the other two have *gauche* bonds near the carboxylic group, giving molecular association to a dimeric structure. In this sense, this series behaves anomalously, since all other metal alkanoates (except those of Rh, Ru, Cr, and W) are ionic bi-layered salts (ionic and lipidic) [3]. In figure 1, a representation of the molecular association and how

---

*Author for correspondence; e-mail: cheda@quim.ucm.es

Liquid Crystals ISSN 0267-8292 print/ISSN 1366-5855 online © 2004 Taylor & Francis Ltd
http://www.tandf.co.uk/journals
DOI: 10.1080/02678290310001628500

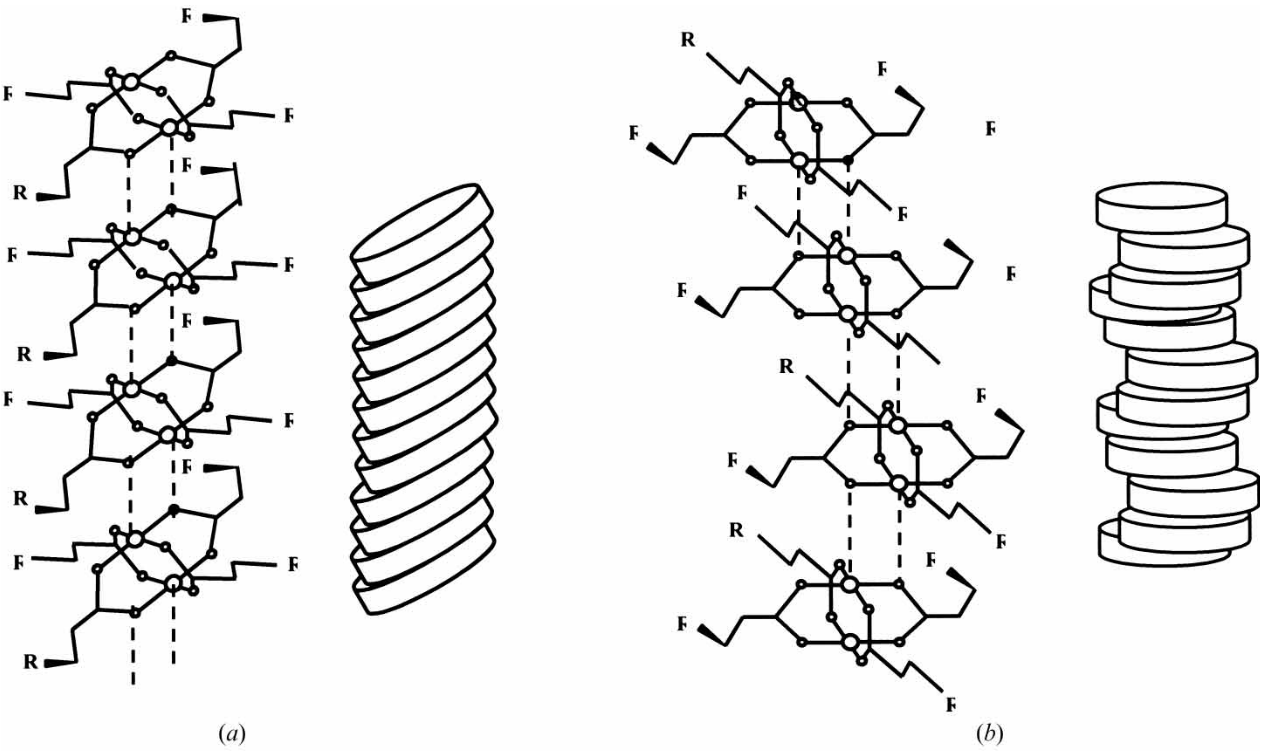

Figure 1. Lantern molecular structure of the di-copper(II) tetra-alkanoates, stacking in the two possible ways for the formation of the columnar phase: (*a*) tilted to the columnar axis, for the tetragonal, (*b*) parallel to the columnar axis, for the hexagonal [9, 12, 14].

the molecules could be stacked is shown in order to better understand not only their molecular shape but also the liquid crystal structure.

Because of the molecular association it is questionable whether or not this family of compounds should be considered as organic salts, and the more appropriate name of di-copper(II) tetra-alkanoates, clearly refers to their molecular structure. On the other hand, one of the methods used to synthesize these materials is indeed an acid–base reaction since the organic acid and copper(II) oxide are the starting reagents.

A rather comprehensive investigation of several copper(II) carboxylates, $Cu(Cn)_2$, with n ranging between 5 and 24 was carried out by Giroud-Godquin, Skoulios and their coworkers by means of various techniques: XRD, optical microscopy and differential scanning calorimetry (DSC) [9, 10], neutron scattering [11] and IR spectroscopy [12] (for $n=6$, 9, 11, 12, 16, 22) at room temperature. Because of the decomposition of the compounds prior to the clearing point, optical microscopy was carried out on the lyotropic columnar phases of the higher members of the series ($n=8$, 12, 18, 20, 22, and 24) by swelling the samples with various organic solvents (hydrocarbons, toluene), finding a first order transition from the columnar discotic to discotic nematic phase, at more dilute concentrations [13, 14]. Mesophases were shown by XRD to be columnar discotic above the butyl homologue. The columns are arranged hexagonally for all the members of the series studied, with the exception of the butanoate, which has a tetragonal (rectangular) array [12].

The FTIR spectra of a series of anhydrous copper(II) carboxylates with $n=6$–10, 12, 14, 16 and 18 were reported by Ramos Moita *et al.* [15], who observed changes in the IR spectra associated with the phase transition from the crystalline to columnar liquid crystal phase. They assigned these changes to modifications in the type of co-ordination around the copper atoms. Redondo *et al.* [16] also observed structural changes related to premelting phenomena in some of these salts. To our knowledge no low frequency infrared or Raman data for the anhydrous shorter members of this series have been published to date. The thermal stability of some of these compounds was investigated by Van My *et al.*, $Cu(C4)_2$ [17], and Bassi *et al.*, $Cu(C3)_2$ and $Cu(C4)_2$ [18].

The present paper reports on the thermophysical properties of the short chain Cu(II) alkanoates with $3 \leqslant n \leqslant 6$, with the aim of determining the existence range of the thermotropic mesophases. Thermal properties were studied by means of DSC and TGA. Hot stage polarizing microscopy was used to identify the columnar phases using a new method based on the findings of Mc Bain [19], Lynch *et al.* [20] and results of our group [21, 22] that have shown that the addition of the corresponding acid to the pure salts enhances the thermal stability, forming homogeneous region of a lyotropic mesophase, in their binary phase diagram, having the same structure as the pure salt.

Variable temperature FTIR and Raman spectroscopic measurements have also been performed to gain a deeper insight into the structures of the solid and mesophases exhibited and the melting process.

2. Experimental

2.1. *Sample preparation*

Experimental difficulties are usually met in the preparation and handling of the short chain linear alkanoates with $n \leqslant 7$, because they are hygroscopic and difficult to crystallize and purify due to their high solubility in polar solvents. The Cu(II) salts studied in this work do not differ in this respect.

As for the synthesis of Cu(II) carboxylates, there is a choice of a variety of chemical reactions [23]. In the present work, the two following methods were adopted:

2.1.1. *Method 1*

This procedure, similar to that described by Bird and Lomer [5], consisted of adding dropwise the *n*-alkanoic acid (propanoic: Fluka puriss. >99.5%; butanoic: Fluka puriss. >99%; pentanoic: Merck-Schchardt zur Synthese >99%; hexanoic: Fluka puriss. >99%) to a hot suspension of basic copper(II) carbonate (Fluka purum p.a. >95%) in excess in absolute ethanol (Fluka puriss. >99.8%), to which some ml of deionized water were also added. After 2–4 days, when evolution of CO_2 was no longer apparent, the hot solution was filtered to remove the excess of carbonate, evaporated to about one half the volume, and allowed to cool to room temperature, thus obtaining the first crystallization of the salt; the flasks then were held 2–3 days at 273 K. The solids obtained were recrystallized three times from ethanol and finally dried under vacuum at about 383 K for 2 h. The products took the form of green–blue powders.

2.1.2. *Method 2*

This method consisted of the direct reaction of copper(II) oxide (Merck pro analysis >99%) with the carboxylic acids (as above, except pentanoic: Fluka puriss. >99.5%) in a small amount of ethanol (C. Erba purum >99.7%) in an Erlenmeyer flask heated under reflux at about 333 K for 2–10 h. From the solutions thus obtained, after a one week rest single crystals, typically about $5 \times 1 \times 0.5\,\mathrm{mm}^3$, could be isolated. After rinsing with ethyl ether, the crystals were dried at 373 K in air for 1 h.

The purities (%) determined by DSC from the enthalpy of fusion to the liquid crystal phase, were 99.98, 99.76 and 99.43 for $Cu(C4)_2$, $Cu(C5)_2$ and $Cu(C6)_2$, respectively. Since its preparation method was the same as for the other members, the purity of $Cu(C3)_2$ must be similar to these values although it could not be determined by DSC because this compound decomposes directly from the crystal phase. The FTIR spectrum of this compound shows no impurity.

2.2. *Optical microscopy*

The photomicrographs shown as figure 2 were obtained by means of a Nikkon polarizing optical microscope (POM), Eclipse E600 Pol, coupled to a digital camera, Hitachi HV-CVO-3CCD. To control the temperature of the samples, a Linkam LTS 350 connected to a TMS94 control was used.

It was not possible to observe textures upon cooling the isotropic melts of the copper (II) carboxylates because of decomposition taking place in the melt. In order to carry out visual observations of the mesophases under the microscope, the technique suggested by Demus and Richter [24] was adopted (evaporating the solvent at a liquid crystal phase temperature of a solution of the sample). Using this method, only a birefringent fluid phase (with no texture) was observed as proof of the liquid crystal phase. Thus a second and definitive method (described later) consisting of the addition of small amounts of the corresponding acid to the pure salt was used.

2.3. *Differential scanning calorimetry and thermogravimetric analysis*

DSC measurements were carried out at the Università di Pavia using a Perkin-Elmer DSC-2 differential scanning calorimeter previously calibrated for temperatures and enthalpies [23]. Samples typically weighed 3–5 mg and were sealed in aluminium pans. Heating rates of $5\text{–}10\,\mathrm{K\,min^{-1}}$ were used, with a dry nitrogen flow of $\sim 30\,\mathrm{ml\,min^{-1}}$. A Seiko Instruments Inc. Model DSC 22 differential scanning calorimeter in connection with the control unit SSC5100 was used at the Universidad Complutense. Tightly sealed aluminium volatile pans, with samples weighing about $(20 \pm 0.001)\,\mathrm{mg}$, were scanned at heating rates of $5\,\mathrm{K\,min^{-1}}$ in air. The instrument was calibrated for temperature using In and Sn samples supplied by Mettler (purity: >99.999% and >99.9%, respectively)

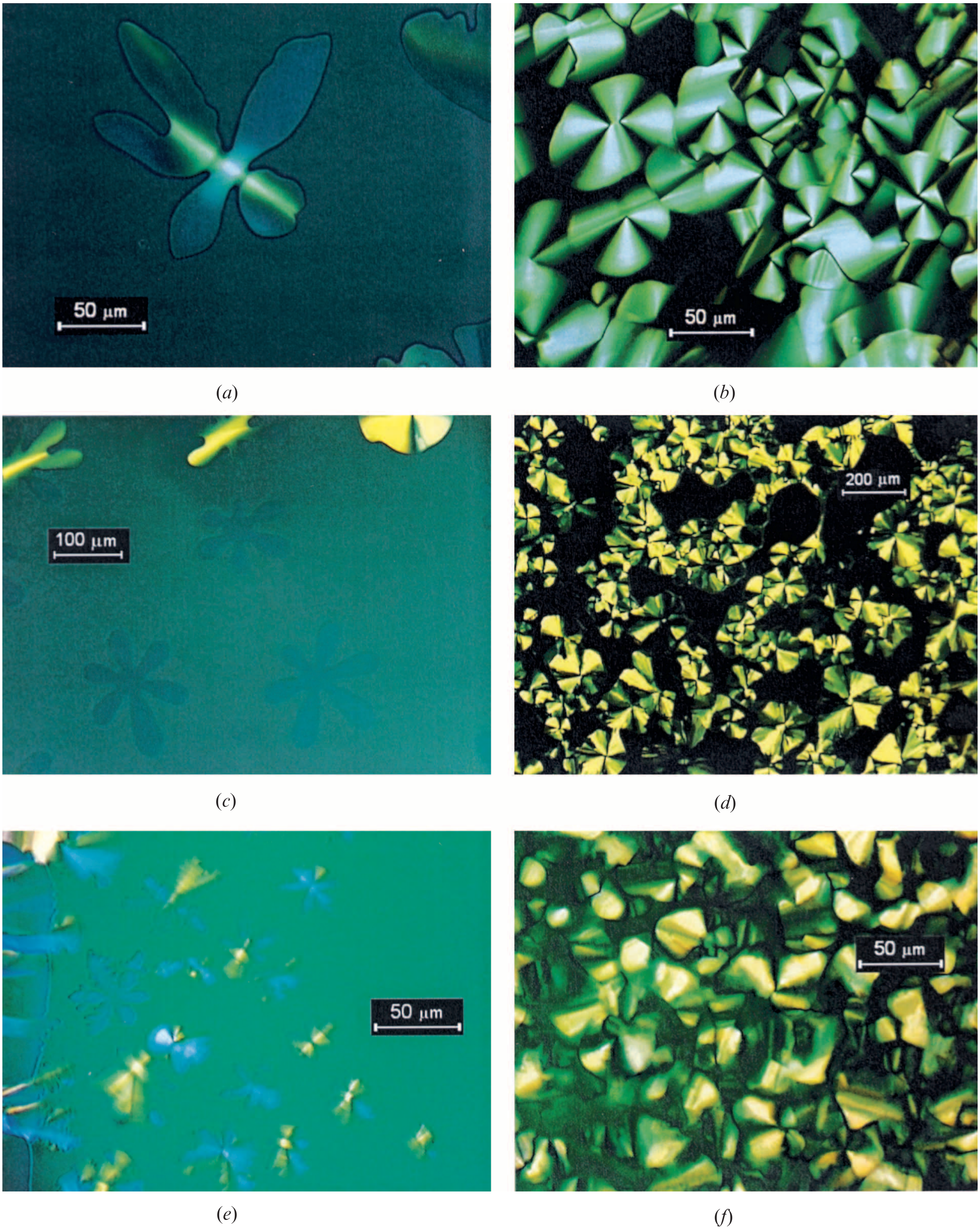

(*a*) (*b*) (*c*) (*d*) (*e*) (*f*)

Figure 2. Copper(II) butanoate: (*a*) tetragonal domains at 184.1°C, uncrossed polars, 20°; (*b*) typical columnar developable domains at 164.7°C, polars rotated +45°. Copper(II) pentanoate: (*c*) hexagonal homeotropic domains at 98.9°C, uncrossed polars, 10°; (*d*) developable domains at 118.9°C, crossed polars, inside isotropic liquid. Copper(II) hexanoate (*e*) hexagonal homeotropic domains, at 135°C, uncrossed polars, 20°; (*f*) developable domains, at 152°C, crossed polars.

and benzoic acid >99.997% supplied by NBS (lot 39i), and for enthalpy with the In and Sn samples described already. The results obtained by means of the two calorimetric techniques were in excellent agreement.

High pressure pans working at an internal pressure of $\leqslant 30$ bar provided by Seiko Inst. Inc. were also used to repeat measurements at higher temperatures when required, i.e. when decomposition phenomena were expected to occur and had to be prevented. Thermogravimetric analysis was carried out using a Du Pont Instruments Thermal Analyst 2000, connected to a Thermogravimetric Analyzer 951. A $2\,\mathrm{L\,h^{-1}}$ nitrogen purge and a heating rate of $10\,\mathrm{K\,min^{-1}}$ were used.

2.4. *FTIR and Raman spectroscopy*

Infrared spectra of the Cu(II) alkanoates in KBr pellets (polyethylene pellets for the far infrared measurements) were recorded using Nicolet 60X, and Nicolet Magna 750 FTIR spectrometers at a resolution of $2\,\mathrm{cm^{-1}}$ in the mid infrared and $4\,\mathrm{cm^{-1}}$ in the far infrared region. A Dilor XY Raman spectrometer with a multichannel detector was used to record the Raman spectra of the materials. The radiation source was an $\mathrm{Ar^+}$ laser at 514.5 nm. However the intensity of the Raman signal was low and also the samples were heated by the laser focused on them. This effect was more pronounced in the shortest members of the series, and as the signal was poorer with rising temperature, it was only possible to obtain Raman spectra at high temperature for copper hexanoate. A commercial variable temperature cell, SPECAC VTL-2, adapted for solid samples was employed to obtain IR and Raman spectra of the heated salts.

Table 1. Thermogravimetric analysis.

Compound	Starting decomposition temperature/K	End of decomposition temperature/K	Residual mass/%[a]
$\mathrm{Cu(C3)_2}$	443	563	18
$\mathrm{Cu(C4)_2}$	423	543	38
$\mathrm{Cu(C5)_2}$	423	563	26
$\mathrm{Cu(C6)_2}$	473	563	26

[a] Approximate values.

3. Results and discussion

3.1. *Optical microscopy*

The slides for microscopic observation were prepared as follows: several microcrystals were spread out on the surface, and heated at about 130°C; a saturated solution of the salt in the acid at the same temperature was poured onto the crystals, and then a cover was put on the sample; this preparation was observed inside a hot stage, and heated and cooled several times, at different rates; domains (hexagonal and tetragonal in shape) appeared on slowly cooling ($0.5\ \mathrm{C\,min^{-1}}$) the whole preparation after heating into the isotropic phase.

Homeotropic tetragonal (for copper butanoate) and hexagonal (for pentanoate and hexanoate) columnar discotic mesophases were clearly observed as shown in figures 2(*a*), 2(*c*), and 2(*e*) (a hexagonal snow-flake-like domain), respectively in figures 2(*b*), 2(*d*) and 2(*f*) developed domains are shown, at specified temperature and magnification, characteristic and unequivocal for columnar phases. These results are in complete agreement with the reported XRD results [9].

To find similarities with the nematic-columnar lyotropic polymesomorphism of the swelled mixtures [13, 14], observations were carried out on several more dilute solutions in acid, with no success. This points to a simpler binary acid–organic salt phase diagram. This method of identifying liquid crystal structures through their textures, consisting of adding the corresponding acid to the metal alkanoate, may be useful not only for salts like these copper(II) alkanoates which decompose before the isotropization temperature, but also in general for all the alkanoic acid salts.

3.2. *TGA*

Results of thermogravimetric analysis are summarized in table 1. In all cases the residual mass is compatible with CuO formation, accompanied by metallic Cu in the case of $\mathrm{Cu(C5)_2}$. These data are in agreement with those reported elsewhere [7, 18].

Table 2. Temperatures and enthalpy changes of the phase transitions for $\mathrm{Cu(C}n\mathrm{)_2}$.

n	$T_{\mathrm{s-s}}$/K	$\Delta_{\mathrm{s-s}}H$/ kJ mol^{-1}	$T_{\mathrm{s-s}}$/K	$\Delta_{\mathrm{s-s}}H$/ kJ mol^{-1}	T_{f}/K	$\Delta_{\mathrm{f}}H$/ kJ mol^{-1}	$\Delta_{\mathrm{tot(S\_S)}}H$/ kJ mol^{-1}	T_{d}/K	$\Delta_{\mathrm{d}}H$/ kJ mol^{-1}
3	421.6	5.200						519.6	12.3
4	395.0	8.273	422.9	1.369	473.1 468[a]	3.210	12.852	542.2	19.190
5					391.0	18.532	18.532	537.7	4.439
6					363.3	17.631	17.631	518.65	6.963

[a] Reference [17].

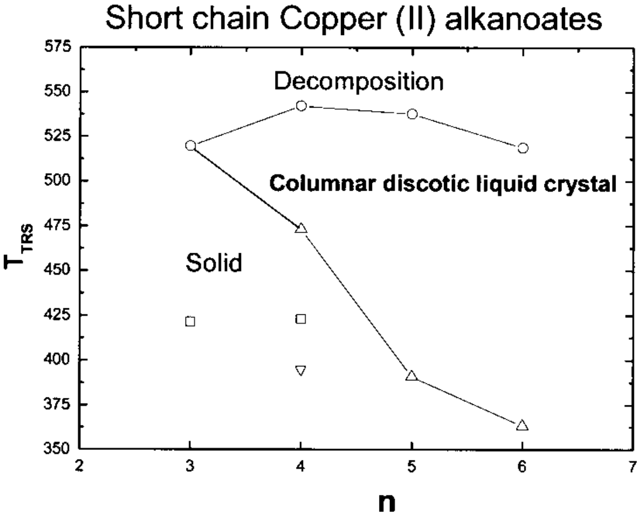

Figure 3. Transition temperatures *vs* number of carbon atoms in the alkanoate chains, Cu(Cn)$_2$. O: decomposition; Δ: fusion; ∇: solid–solid transitions.

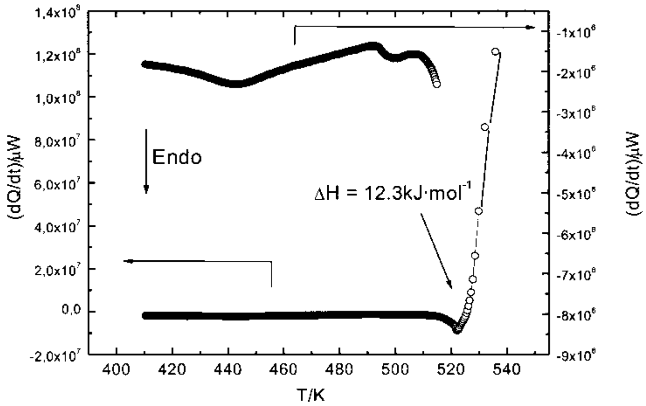

Figure 4. Thermogram of Cu(C3)$_2$ recorded in a high pressure volatile pan.

3.3. *DSC*

The agreement of the results obtained from the two different calorimeters used for samples of the same compound, independent of the synthesis method, is very good and within experimental error, thus confirming data reliability. The temperatures and associated enthalpy changes of the phase transitions for the copper carboxylates studied in this work are shown in table 2. These data are the average of all the measurements (at least two) on each of the two different samples of the different compounds.

All the compounds studied show a liquid crystal phase, except for the shortest member, Cu(C3)$_2$, which decomposes directly from the crystal, see figure 3. This decomposition (already measured by TGA) has also been observed by DSC using a high pressure pan to record the thermogram. Figure 3 shows that the longer the alkyl chain the lower is the temperature at which the mesophase appears. However the decomposition temperature is practically constant for all the members. The thermal behavior of each particular compound is described below.

3.3.1. *Copper(II) propanoate*

A small endothermic broad peak between 421.6 and 470 K (with a maximum at about 444 K) together with a small thermal anomaly prior to the endothermic decomposition are seen, (see upper part of figure 4). No isotropic liquid was observed in the sample under POM confirming that the shoulder does not correspond to a melting to liquid nor to a liquid crystal. Sample decomposition takes place at higher temperature, initiating at 503 K as an endothermic process followed by an exothermic one starting at about 520 K.

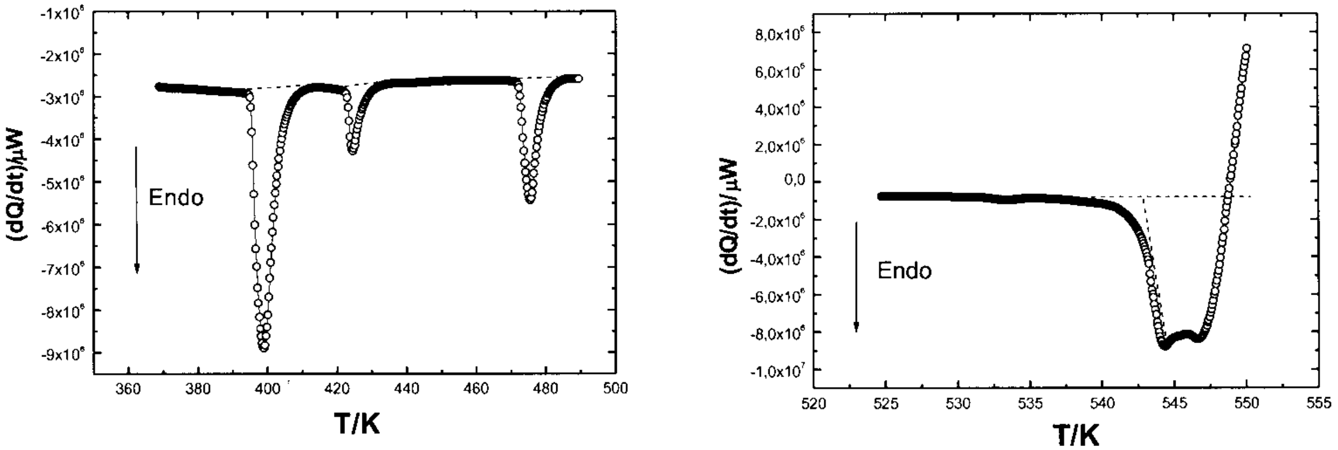

(*a*) (*b*)

Figure 5. Thermogram of Cu(C4)$_2$: (*a*) complete thermogram, (*b*) decomposition recorded in a high pressure volatile pan.

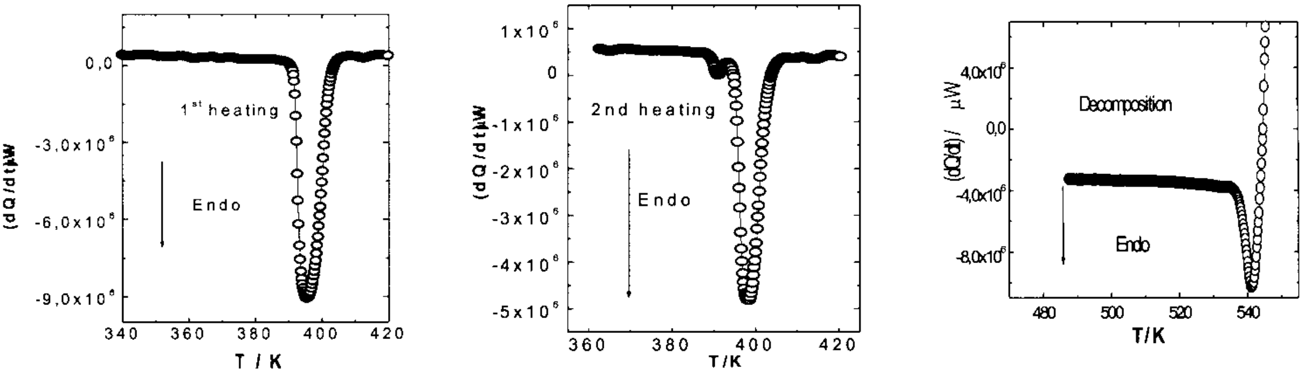

(*a*) (*b*) (*c*)

Figure 6. Thermogram of $Cu(C5)_2$: (*a*) first heating, (*b*) second heating recorded immediately after the sample solidified from the melt, (*c*) decomposition recorded in a high pressure volatile pan.

We have observed that copper(II) propanoate sublimes when heated in vacuum above the maximum temperature of the shoulder at about 440 K. This may be explained in terms of the molecular nature of the crystal, due to the di-copper(II) tetra-alkanoate molecular association. This fact gives an added interest to this compound as a potential precursor of copper and copper oxide particles by chemical vapor deposition methods [25].

The only thermal data found for this compound in the literature are in [18], where it is reported that the crystal structure persists for this compound until thermal decomposition, with no mention of temperature; and [23], where the hemihydrated copper propionate is studied by DTA and TG. In this work the authors found only an exothermic decomposition in three steps at 533, 603 and 703 K for the anhydrous sample without detecting the lower temperature endothermic decomposition reported here.

3.3.2. *Copper(II) butanoate*

Two solid–solid transitions were observed prior to the fusion of the crystal to a liquid crystal phase which were not reported by Ibn-Elhaj *et al.* [10], or by van My *et al.* [17], where only the fusion to the mesophase is reported; see figure 5 (*a*). There is no doubt about the existence of these two solid–solid transitions because they were observed in several samples prepared by the two different methods indicated above. Variable temperature FTIR spectroscopy also reveals changes at these temperatures, thus confirming the existence of these solid phases. Sample decomposition takes place immediately after fusion as shown in figure 5 (*b*).

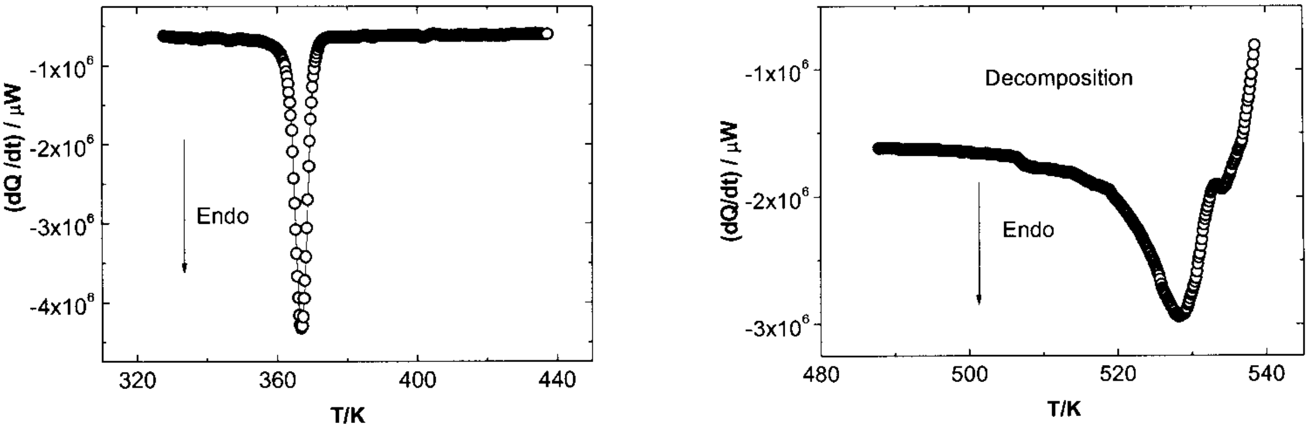

(*a*) (*b*)

Figure 7. Thermogram of $Cu(C6)_2$: (*a*) complete thermogram, (*b*) decomposition recorded in a high pressure volatile pan.

3.3.3. *Copper(II) pentanoate*

The thermal behaviour of this salt is characterized by the presence of a single peak in the first heating, figure 6 (*a*), that splits into two peaks at different temperatures in the second heating when recorded immediately after sample crystallization from the melt, figure 6 (*b*). The area under the peaks is dependent on the time elapsed between consecutive thermograms. This can be explained by considering that the solid phase obtained from the melt is metastable and transforms into the thermodynamically more stable initial phase, after a certain period of time. This is confirmed by the third heating cycle obtained after two days, which is practically identical to the first. The transition temperature is some degrees higher than that reported previously [10] but its enthalpy is considerably higher, pointing to a higher purity of our samples. To our knowledge no data for the

Table 3. Infrared peaks (cm^{-1}) and assignments: ν stretching; δ bending; γ torsion; w wagging; tw twisting.

$\mathrm{Cu(C3)_2}$	$\mathrm{Cu(C4)_2}$	$\mathrm{Cu(C5)_2}$	$\mathrm{Cu(C6)_2}$	Assignment
2983(sh), 2974s	2963s	2964(sh), 2956s	2954s	$\nu_{as}(\mathrm{CH_3})$
2942s, 2920s	2933m	2931ss	2931s	$\nu_{s}(\mathrm{CH_3})$
2879m-w	2874m	2872m	2872m	$\nu_{as}(\mathrm{CH_2})$
2850m-w		2862(sh)	2860m, 2853(sh)	$\nu_{s}(\mathrm{CH_2})$
1622(sh)				
1589vs	1587vs	1586vs	1588vs	$\nu_{as}(\mathrm{COO^-})$
1512w	1513w	1510w	1510w	
1474m-w		1469m-w	1468m-w	$\delta_{as}(\mathrm{CH_3})$
1460m-w	1463m	1461m-w	1453m-w	$\delta_{as}(\mathrm{CH_3})$
		1449m-w		$\delta_{as}(\mathrm{CH_3})$
1441sh	1430s	1432m	1432m	$\delta(\mathrm{CH_2})$
1426s	1421s	1416m	1416m	$\nu_{s}(\mathrm{COO^-})$
	1415(sh)	1408(sh)	1406(sh)	
1382w, 1372w	1379m-w	1374w	1378w	$\delta_{s}(\mathrm{CH_3})$
		1362m	1367w	$\delta_{s}(\mathrm{CH_3})$
	1347m		1345m	w $(\mathrm{CH_2})$
	1317m	1319m	1313m	w $(\mathrm{CH_2})$
1303m		1297m	1294m-w	w $(\mathrm{CH_2})$
	1265m		1279vw, 1272vw	tw $(\mathrm{CH_2})$
	1261w	1243m		
	1243w	1228m-w	1230m	tw $(\mathrm{CH_2})$
		1201m	1212m-w	tw $(\mathrm{CH_2})$
		1180(sh)	1192m	tw $(\mathrm{CH_2})$
1087m	1105m	1110m	1111m	$\nu\ (\mathrm{CC_\alpha})$
1080m, 1074sh	1079w, sh	1095m-w		
		1064vw	1060(sh), 1053vw	$\gamma\ (\mathrm{CH_3})$
	1051w, 1040sh	1050vw		$\gamma\ (\mathrm{CH_3})$
	1040w	1026vw	1035vw	$\gamma\ (\mathrm{CH_3})$
1015w			1009vw	$\gamma\ (\mathrm{CH_3})$
1000sh, vw		1000vw	1001vw	$\nu\ (\mathrm{CC})$
	958vw	952w	959vw	$\nu\ (\mathrm{CC})$
	933vw	937w		$\nu\ (\mathrm{CC})$
		926w	920w	$\nu\ (\mathrm{CC})$
893m	899w–m	899w	892w	$\nu\ (\mathrm{C_\alpha\ CO})$
	874w	881vw	876vw	$\nu\ (\mathrm{C_\alpha\ CO})$
		863w	864vw	$\nu\ (\mathrm{C_\alpha\ CO})$
		837w	847w	
811m, 799(sh)	801m	804w	805w	$\gamma\ (\mathrm{C_\alpha H_2})$
756vw	754m	767m-w	763w	$\gamma\ (\mathrm{CH_2})$
	732m	730(sh)		$\gamma\ (\mathrm{CH_2})$
		723m	725m	$\gamma\ (\mathrm{CH_2})$
699w	706w			
667m	654m	670m	668m	$\delta\ (\mathrm{COO^-})$
597w, 566w	605w, 563w	594w, 577w, sh	589w	$\gamma\ (\mathrm{COO^-})$
529w	527w	532w	535w	$\pi\ (\mathrm{COO^-})$
	427m	450m-w	452m-w	$\delta\ (\mathrm{CCC})$
		415m	434m.w	$\delta\ (\mathrm{CCC})$

endothermic decomposition transition exists in the literature for comparison.

3.3.4. *Copper(II) hexanoate*

Only the transition corresponding to the melting to the liquid crystal phase is observed, figure 7 (*a*), for this homologue apart from the decomposition reported for all the compounds. The transition temperature is some degrees lower and the enthalpy higher than the values previously reported for this compound [10]. This process takes place in two steps, an endothermic transition first, which in most cases does not finish because an irreversible exothermic transition occurs immediately after this effect, see figure 7 (*b*).

3.4. *Infrared and Raman spectra*

Mid-infrared spectra of copper propanoate and hexanoate (the shortest and the longest of the compounds studied in this work) at room temperature, are shown in figure 8. The positions of the bands seen in the IR spectra of the four compounds studied, with their assignments, are listed in table 3. As can be seen, the IR spectrum of our sample of copper hexanoate is very similar to that reported by Ramos-Moita *et al.* [15] although some bands assigned by these authors to CH_2 and CH_3 vibrations are absent from our spectrum. The origin of these small differences in the infrared spectrum must be the reported ability [16] of these compounds to adopt different forms (poly-types) at room temperature depending on their previous history, in a similar way to that observed in fatty acids [26].

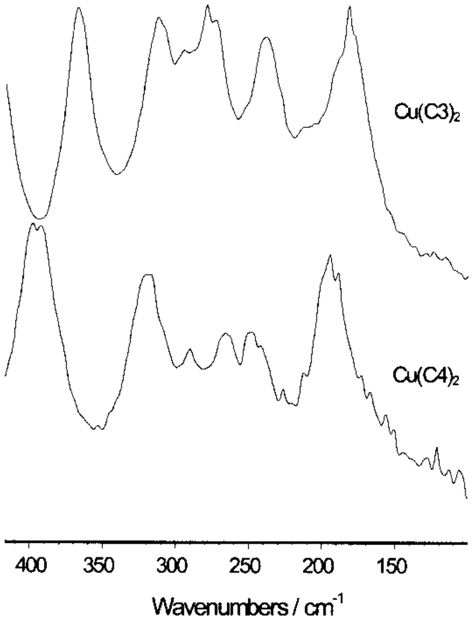

Figure 9. Far-infrared spectra of copper propanoate and butanoate.

As expected, the infrared spectra of all the compounds studied are very similar: they show bands

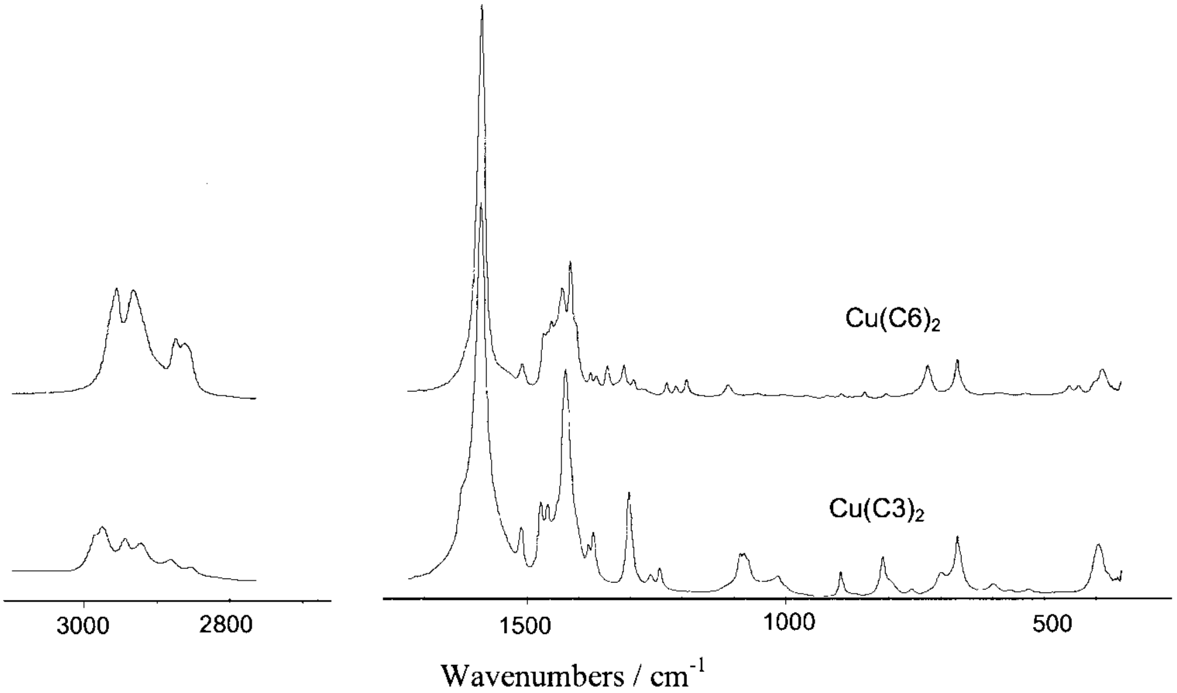

Figure 8. Mid-infrared spectra of copper propanoate and hexanoate.

ascribed to the carboxylate groups and some others due to vibrations of the alkyl chain. The frequency of the asymmetric (about 1 585 $\mathrm{cm^{-1}}$) and symmetric $\mathrm{COO^-}$ (about 1 420 $\mathrm{cm^{-1}}$) stretches correspond to the same bridging bidentate coordination present in all the members of the series. Some features of the IR spectrum of copper propanoate deserve a comment: firstly, the relative intensity of bands assigned to $\mathrm{COO^-}$

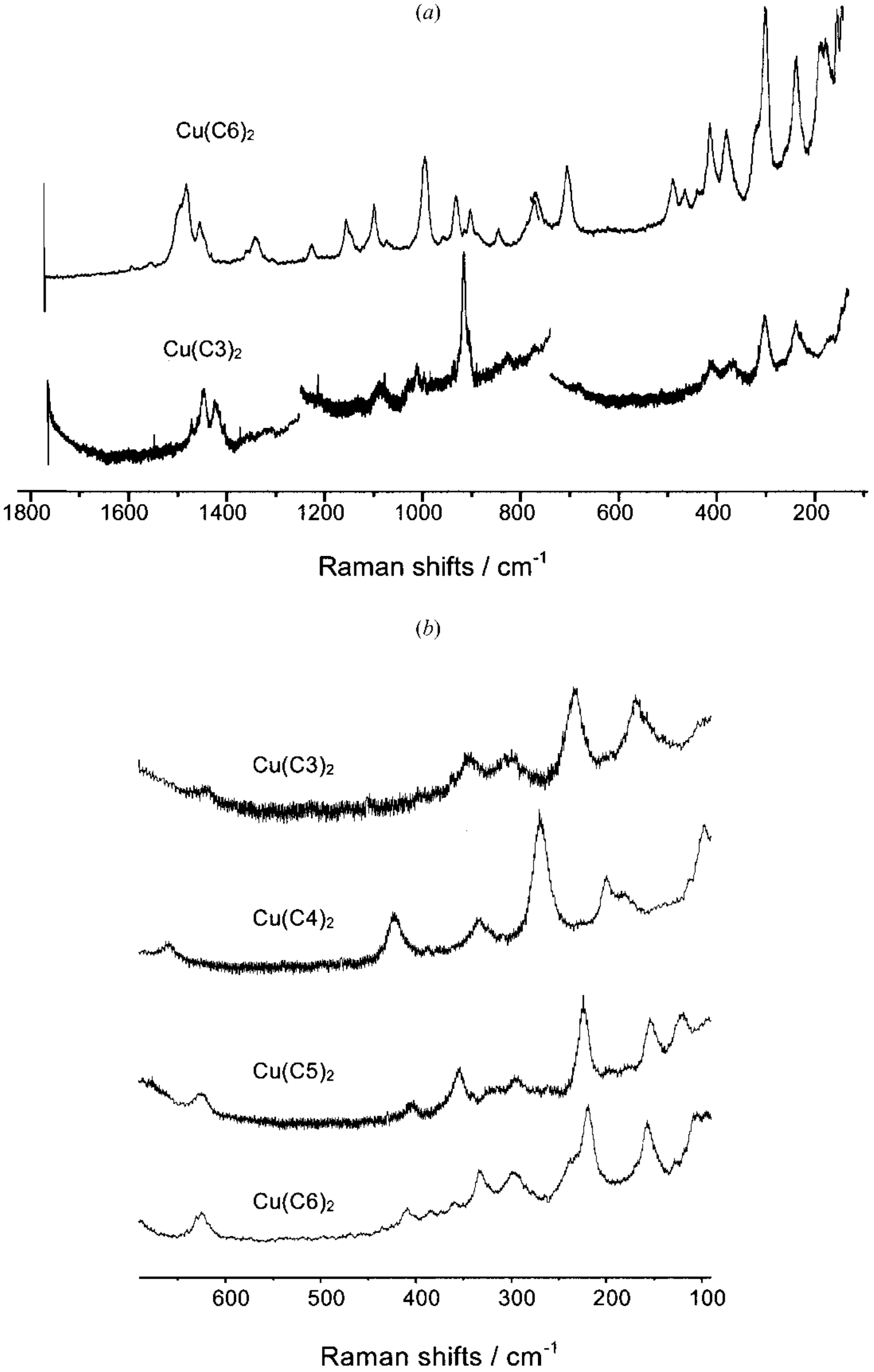

Figure 10. (*a*) Raman spectra of copper propanoate and hexanoate; (*b*) low frequency Raman spectra of $\mathrm{Cu(Cn)_2}$, $n=3$ to 6.

group vibrations is higher than in the longer chain compounds; secondly, many of the bands due to CH_2 and CH_3 vibrations are split into two components; finally, the wavenumbers of CH_2 vibrations are shifted significantly with respect to those of corresponding bands in the other members of the series. All these features have the same origin: the existence of only one methylene group in the propanoate chain which, in addition, rules out the possibility of progression bands. These and other spectral features will be discussed along with the variable temperature spectra.

Particular attention has been paid to the far-infrared region where bands associated with the ionic central disc are observed. The far-infrared spectra of all the compounds studied are very similar and only minor changes in band frequencies are seen. For example, the spectra of $Cu(C3)_2$ and $Cu(C4)_2$ in the region between 400 and $100\,cm^{-1}$ can be seen in figure 9.

The Raman spectra of copper propanoate and hexanoate between 1800 and $100\,cm^{-1}$ are shown in figure 10 (*a*). The observed high width of some bands and the high noise level clearly indicate the heating effect described in the experimental section. In figure 10 (*b*), Raman spectra of the low frequency region (in which the heating effect is less pronounced) for all the compounds studied are shown. Wavenumbers of Raman and infrared bands in this region are compared in table 4. No coincident bands in the two spectra are observed, confirming that the D_{4h} symmetry of the central ionic core in the crystal phase is common for all the compounds of the series [5–8] and that the conformation of the chains does not appreciably affect this symmetry.

The vibrational spectra of the compounds studied change with temperature, the most remarkable variation being observed at temperatures coincident with that of some of the phase transitions as determined by DSC. Copper propanoate is the only compound without a mesophase. It shows a phase transition at 421.6 K followed by decomposition of the sample. At that temperature the splitting observed in some infrared bands assigned to CH vibrations disappears (see figure 11), the two COO^- rocking bands coalesce at $587\,cm^{-1}$ and a new band at about $542\,cm^{-1}$ attributable to the COO^- wagging vibration appears. According to Zerbi *et al.* [27] these changes in carboxylate out-of-plane vibrations are related to the conformation of the alkyl chains with respect to the COO^- group. Therefore all the changes observed can be explained if 'free' rotational movements can take place within the alkyl chains. In other words, prior to the decomposition of copper propanoate a transition from crystal to a new phase, in which the chains are in a liquid-like state, takes place at the temperature indicated.

As already discussed, the thermal behaviour of $Cu(C4)_2$ is very different from the rest of the samples. Mid-FTIR spectra collected at 25, 130, 160 and 200°C are shown in figure 12 (*a*). These spectra, which correspond to the different phases observed for this compound, show significant differences in the bands assigned to the alkyl chain vibrations and to the carboxylate group. However the most important changes take place in the first solid–solid transition and seem to be related to increasing conformational disorder of the alkyl chain. In the solid III to mesophase transition the growth of the band at about $1540\,cm^{-1}$ and the absence of the band at about $1515\,cm^{-1}$ are the most noticeable features. These changes in the carboxylic band range at the mesophase transition are common to all the Cu(II) carboxylates (with only the exception of the propanoate member for which no mesophase exists) and have been

Table 4. Low frequency infrared and Raman peaks (cm^{-1}): ν stretching; δ bending.

$Cu(C3)_2$		$Cu(C4)_2$		$Cu(C5)_2$		$Cu(C6)_2$		Assignment
IR	Raman	IR	Raman	IR	Raman	IR	Raman	Mathey *et al.* [28]
395		368			396		399	ν(Cu–O)
	384		329	394		387		ν(Cu–O)
	343	313			374		373	ν(Cu–O)
319		295			337	341		ν(Cu–O)
291		280		307			337	δ(Cu–Cu–O)
	273		265	288		301		δ(Cu–Cu–O)
268					266		277	δ(Cu–Cu–O)
				259			261	δ(Cu–Cu–O)
250		239		242		232		δ(O–Cu–O)
	209		197	213		213		δ(O–Cu–O)
196		182			197		199	δ(O–Cu–O)
	134		178		164		138	δ(O–Cu–O)

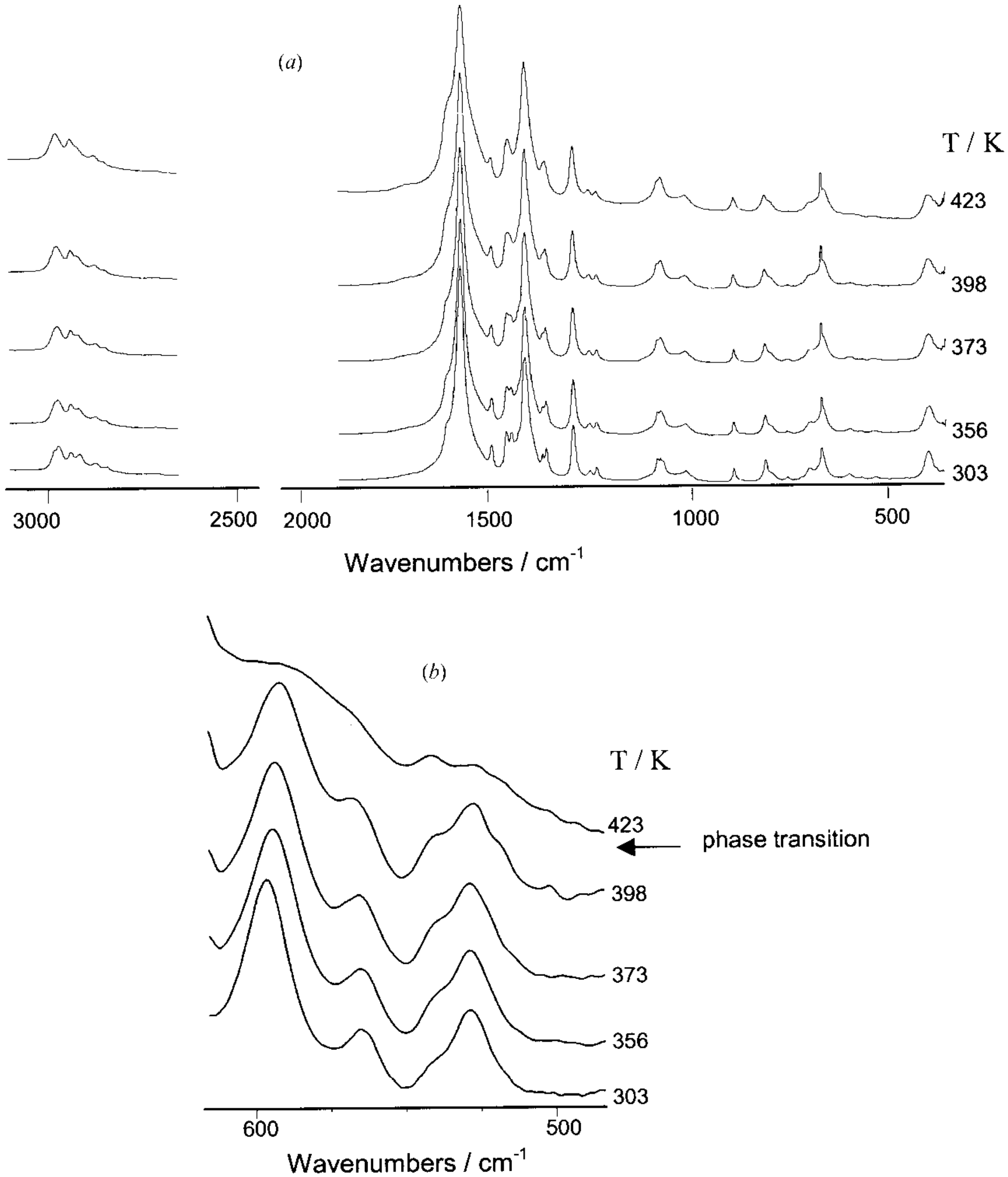

Figure 11. (*a*) Mid-infrared spectra of Cu(C3)$_2$ at different temperatures; (*b*) magnification of the 625–500 cm^{-1} region.

interpreted [15] as due to a change in the coordination type.

The far-infrared spectrum of Cu(C4)$_2$ is very sensitive to temperature, figure 12 (*b*). At the first solid–solid transition (395 K), the bands assigned to Cu–O stretches at 368 and 313 cm^{-1} [28] decrease in intensity while Cu–Cu–O deformation modes increase and O–Cu–O deformations remain. This implies that the geometry of the central core is also involved in this solid–solid transition. Because the far-infrared spectra were recorded using a sample dispersed in a polyethylene matrix, it was not possible to increase the temperature above 145°C, hence a study of the other phase transitions could not be performed.

Changes in the infrared spectra of copper pentanoate and hexanoate are observed at the solid to mesophase transition which is the only transition observed for these compounds before sample decomposition. At that

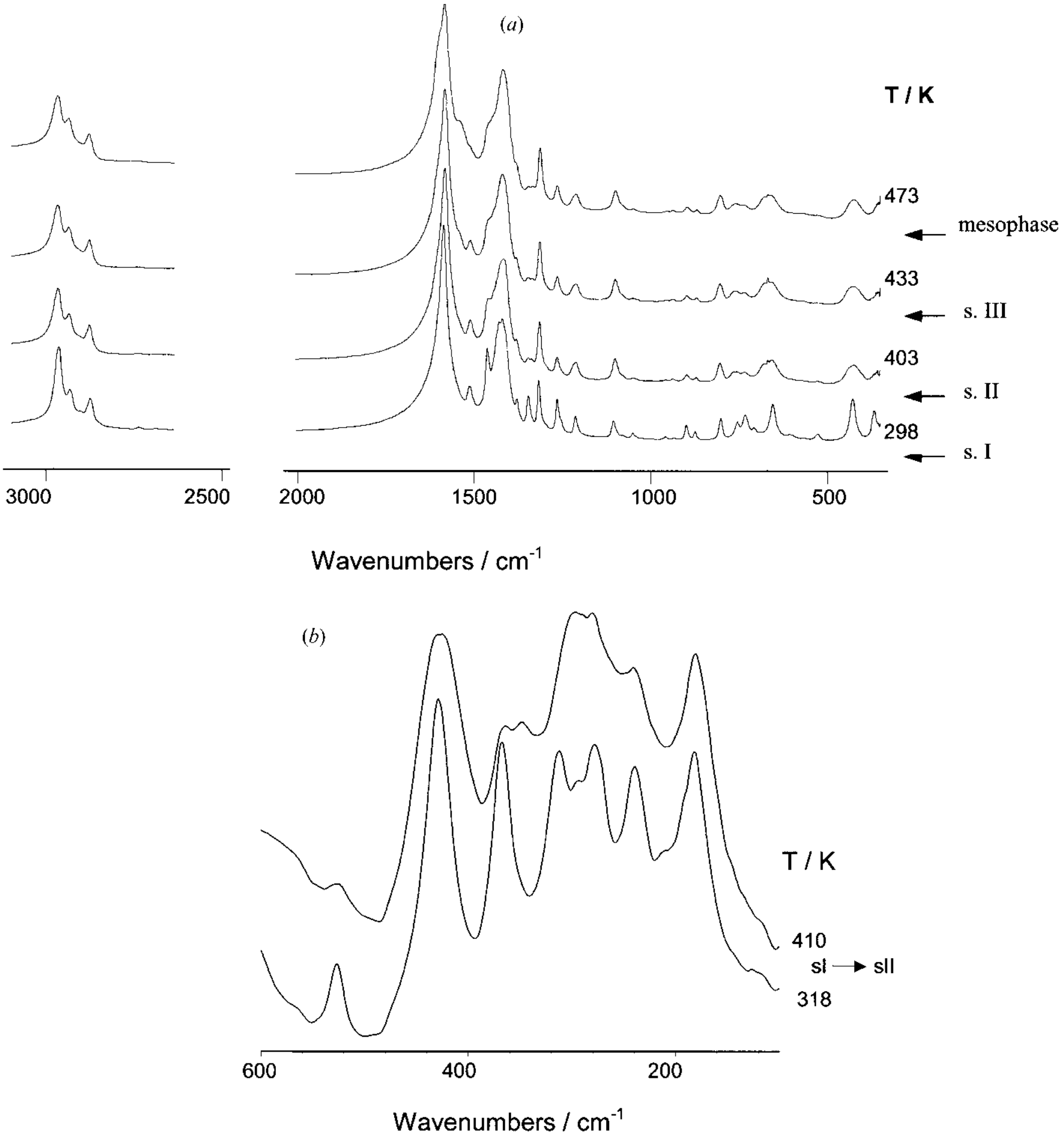

Figure 12. Infrared spectra of $Cu(C_4)_2$ at various temperatures: (*a*) mid-infrared region, (*b*) far-infrared region.

temperature significant changes occur in the bands assigned to carboxylate group vibrations, similar to those observed in the copper butanoate spectrum at the same phase transition. In addition, the frequency and/or intensity of some of the bands corresponding to C–H stretching, bending, rocking and wagging vibrations vary. As an example, the infrared spectra of copper pentanoate at different temperatures are shown in figure 13.

These features suggest that the mesophase structure must be the same as that proposed by Ramos Moita *et al.* [15*a*] for long chain Cu(II) carboxylates since the observed spectral changes in the 4000–600 cm^{-1} range follow the same pattern as that described by these authors. The study of the 600–150 cm^{-1} region confirms that important changes of the binuclear copper central core take place in the mesophase. For $Cu(C5)_2$ and $Cu(C6)_2$, where no additional solid–solid transition

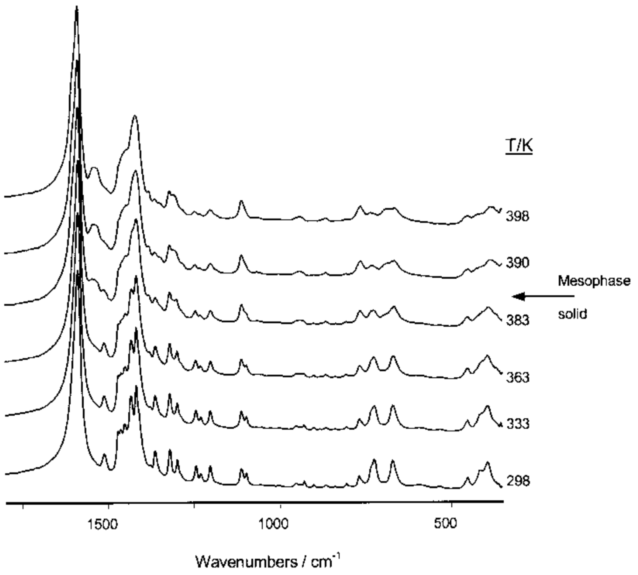

Figure 13. Infrared spectra of $Cu(C_5)_2$ at various temperature.

exists, conformational disorder in the alkyl chains also plays an important role in their solid to mesophase transitions. As stated already, in $Cu(C4)_2$ conformational disorder is related to the first solid–solid transition, but the infrared spectrum of this compound in the mesophase shows the same features common to all the compounds studied.

Partial support of this research by the DGICYT of the Spanish Ministerio de Educación, Cultura y Deportes (Project BQU2001–2021) is gratefully acknowledged. The authors wish also to thank Prof. O. D. Lavrentovich (Liquid Crystal Institute, Kent State University, Kent. OH, US) for providing experimental facilities during the stay of one of us (J.A.R. C.), grant in aid by the Spanish Ministerio de Educación, Cultura y Deportes.

References

[1] FRANZOSINI, P., SANESI, M. (editors), 1980, *Thermodynamic and Transport Properties of Organic Salts* (Oxford: Pergamon Press).

[2] MIRNAYA, T. A., PRISYAZHNY, V. D., and SHCHERBAKOV, V. A., 1989, *Russ. chem. Rev.*, **58,** 821.

[3] DONNIO, B., 2002, *Curr. Opin. Colloid Interface Sci.*, **7,** 371.

[4] MROZINSKI, J., HEYDUK, E., and KORABIK, M., 1994, *Bull. Polish Acad. Chem.*, **42,** 169 and references therein.

[5] BIRD, M. J., and LOMER, T. R., 1972, *Acta Cryst. B*, **28,** 244.

[6] CAMPBELL, G. C., and HAW, J. F., 1988, *Inorg. Chem.*, **27,** 3706.

[7] DOYLE, A., FELCMAN, J., PRADO GAMBARDELLA, M. T., NAZARI VERANI, C., and BRAGANÇA TRISTAO, M. L., 2000, *Polyhedron*, **19,** 2621.

[8] (*a*) LOMER, T. R., and PERERA, K., 1974, *Acta Cryst. B*, **30,** 2913; (*b*) LOMER, T. R., and PERERA, K., 1974, *Acta Cryst. B*, **30,** 2912.

[9] ABIED, H., GUILLON, D., SKOULIOS, A., WEBER, P., GIROUD-GODQUIN, A. M., and MARCHON, J. C., 1987, *Liq. Cryst.*, **2,** 269.

[10] IBN-ELHAJ, M., GUILLON, D., SKOULIOS, A., GIROUD-GODQUIN, G. A. M., and MALDIVI, P., 1992, *Liq. Cryst.*, **13,** 731.

[11] GIROUD-GODQUIN, A. M., MALDIVI, P., MARCHON, J. C., BÉE, M., and CARPENTIER, L., 1989, *Mol. Phys.*, **68,** 1353.

[12] STROMMEN, D. P., GIROUD-GODQUIN, A. M., MALDIVI, P, and MARCHON, J. C., 1987, *Liq. Cryst.*, **2,** 689.

[13] SEGHROUCHNI, R., and SKOULIOS, A., 1995, *J. Phys. II Fr.*, **5,** 1385.

[14] IBN-ELHAJ, M., GUILLON, D., SKOULIOS, A., GIROUD-GODQUIN, A. M., and MARCHON, J. C., 1992, *J. Phys. II Fr.*, **2,** 2197.

[15] (*a*) RAMOS MOITA, M. F., DUARTE, M. L. T. S., and FAUSTO, R., 1994, *J. Chem. Soc. Faraday Trans.*, **90,** 2953; (*b*) FAUSTO, R., RAMOS MOITA, M. F., and DUARTE, M. L. T. S., 1995, *J. mol. Struct.*, **349,** 439.

[16] REDONDO, M. I., GARCÍA, M. V., GONZÁLEZ-TEJERA, M. J., and CHEDA, J. A. R., 1995, *Spectrochim. Acta.*, **51A,** 341.

[17] (*a*) VAN MY, L., PERINET, G., and BIANCO, P., 1966, *Bull. Soc. Chim. Fr.*, **10,** 3104; (*b*) VAN MY, L., and PERINET, G., 1966, *Bull. Soc. Chim. Fr.*, **10,** 3109.

[18] (*a*) KALSI, P. C., BASSI, P. S., and KHAJURIA, C. M., 1980, *Thermochim. Acta*, **41,** 265; (*b*) BASSI, P. S., JAMWAL, H. S., and RANDHAWA, B. S., 1983, *Thermochim. Acta*, **71,** 15.

[19] MCBAIN, J. W., and STEWART, A., 1933, *J. phys. Chem.*, **37,** 924.

[20] LYNCH, M. L., PAN, Y., and LAUGHLIN, R. G., 1996, *J. phys. Chem.*, **100,** 357.

[21] CHEDA, J. A. R., FERNÁNDEZ-GARCÍA, M., FERLONI, P., and FERNÁNDEZ-MARTÍN, F., 1991, *J. chem. Thermodyn.*, **23,** 495.

[22] CHEDA, J. A. R., FERNÁNDEZ-GARCÍA, M., UNGARELLI, P, FERNÁNDEZ-MARTÍN, F., and FERLONI, P., 2000, *Langmuir*, **16,** 5825.

[23] YODER, C. H., SMITH, W. D., KATOLIK, V. L., HESS, K. R., THOMSEN, M. W., YODER, C. S., and BULLOCK, E. R., 1995, *J. chem. Educ.*, **72,** 267.

[24] DEMUS, D., and RICHTER, L., 1978, *Textures of Liquid Crystals* (Berlin: Verlag Chemie), p. 92.

[25] NASIBULIN, A. G., KAUPPINEN, E. I., BROWN, D. P., and JOKINIEMI, J. K., 2001, *J. phys. Chem. B*, **105,** 11067.

[26] SATO, K., and KOBAYASHI, W., 1991, *Crystals, Growth, Properties and Applications: Organic Crystals.*, Vol. 1, edited by N. Kare (Springer-Verlag), pp. 65–108.

[27] ZERBI, G., MINONI, G., and TULLOCH, A. P., 1983, *J. Chem. Phys.*, **78,** 5853.

[28] MATHEY, I., GREIG, D. R., and SHRIBER, D. F., 1982, *Inorg. Chem.*, **21,** 3409.